

WIND-ERODED FLOOR DEPOSITS IN NOACHIAN DEGRADED CRATERS ON MARS. R. P. Irwin III^{1,2}, F. Pendrill³, T. A. Maxwell², A. D. Howard⁴, and R. A. Craddock², ¹Planetary Science Institute, 1700 E. Ft. Lowell Rd., Suite 106, Tucson, AZ 85719, irwin@psi.edu. ²Center for Earth and Planetary Studies, National Air and Space Museum, Smithsonian Institution, MRC 315, 6th St. at Independence Ave. SW, Washington DC 20013-7012. ³University of Gothenburg, SE-405 30, Gothenburg, Sweden. ⁴Department of Environmental Sciences, University of Virginia, Charlottesville VA 22904.

Introduction: The role of water in Noachian crater degradation is key to understanding the paleoclimate of early Mars. Most global- to regional-scale geologic maps suggested widespread volcanic resurfacing of impact crater floors in the early Hesperian [1,2]. Large degraded craters often have flat floors that are consistent with volcanic resurfacing, as the Mars Exploration Rover Spirit found in Gusev crater [3]. Many Noachian craters regardless of size have floors with high thermal inertia [4]. However, the topography of degraded crater rims and interior deposits indicates a dominant role for fluvial erosion and deposition, particularly in craters <60 km in diameter [5,6].

We examined >1000 floors of Noachian craters from 0–30°S, 0–165°E to identify friable deposits that (unlike basalts) were susceptible to aeolian deflation. We used visible-wavelength orbital imaging at 0.25–18 m/pixel from the High Resolution Imaging Science Experiment, Mars Orbiter Camera, Context Camera, and Thermal Emission Imaging System.

Erosional Resistance of Crater Floors: The morphology of Noachian crater floors varies greatly, suggesting diverse fill materials and/or weathering and erosion processes [7]. Some floor materials retain abundant small, post-depositional craters, but they are otherwise smooth. At the opposite extreme are knobby floors (Fig. 1), some of which have exposed layers. In many cases we noted light-toned, seemingly friable material overlain by a more resistant, darker unit. During post-depositional modification, deflation of the darker-toned surface layer removes much of the small-crater population and may expose the underlying light-toned layer, whereas less effective deflation leaves patchy exposures of deeper materials. These friable, wind-eroded deposits are confined to the floors of craters and intercrater basins.

Spatial Distribution of Wind-eroded Crater Floors: Knobby, deflated crater floors are concentrated in a southern band within the study area, except between 60–90°E, where we found no north-to-south increase in floor erosion. Light-toned outcrops on basin floors are concentrated south of 20°S. The area from 20–25°S, 25–100°E contains about a third of the outcrops of light-toned material in the study area, with concentrations near the rim of Hellas and southwest of Huygens crater (~20–25°S, 40–50°E). The observed

concentration of fracturing in light-toned outcrops in these areas may be due to better image coverage.

Discussion: Possible reasons for the diverse Noachian crater-floor morphology are: 1) different resurfacing processes around the Noachian/Hesperian transition; 2) different intensity of post-Noachian aeolian modification; and/or 3) different surface weathering rates, possibly related to material properties. The concentration of knobby terrain and light-toned layers in crater or intercrater basins suggests that these units are not an airfall mantle, and that any enhanced weathering processes must have been focused in the basins. Wind-eroded crater floors appear concentrated in low-albedo, dust-free regions, so increased aeolian efficiency may be partly responsible.

Conclusions: Many Noachian craters have friable, wind-eroded deposits restricted to their floors, some with deeper light-toned material exposed, suggesting aqueous depositional environments. These craters are concentrated in low-albedo, dust-free highland regions. In many cases, basaltic volcanism was not the last significant resurfacing process in these craters.

References: [1] Scott D. H. and Carr M. H. (1978) USGS Map I-1083. [2] Scott D. H. et al. (1986–1987) USGS Map I-1802. [3] Arvidson R. A. et al. (2006) *JGR*, 111, E02S01, doi:10.1029/2005JE002499. [4] Putzig N. E. and Mellon M. T. (2007) *Icarus*, 191, 68–94. [5] Craddock R. A. et al. (1997) *JGR*, 102, 13,321–13,340. [6] Craddock R. A. and Howard A. D. (2002) *JGR*, 107(E11), 5111, DOI:10.1029/2001JE001505. [7] Irwin R. P. et al. (2009) *LPSC* 40, 2358.

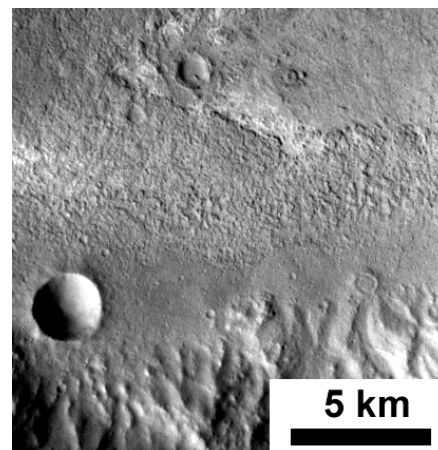


Fig. 1. Gullied Noachian crater wall and etched floor, THEMIS V07923006, 28.1°S, 129.8°E.